

## THE H+D<sub>2</sub> REACTION: HD( $v=1, J$ ) AND HD( $v=2, J$ ) DISTRIBUTIONS AT A COLLISION ENERGY OF 1.3 eV

Richard S. BLAKE<sup>1</sup>, Klaus-Dieter RINNEN, Dahv A.V. KLINER and Richard N. ZARE

*Department of Chemistry, Stanford University, Stanford, CA 94305, USA*

Received 14 November 1988

Complete quantum state distributions for HD( $v=1$ ) and HD( $v=2$ ) are obtained by photolyzing HI at 266 nm in the presence of D<sub>2</sub> and detecting the nascent HD product via (2+1) resonance-enhanced multiphoton ionization (REMPI). Calibration against an effusive oven source ( $\leq 1800$  K) yields any necessary correction factors to relate the integrated ion signals to relative quantum state populations. Comparisons are made with previously published experimental results of Gerrity and Valentini and of Marinero, Rettner and Zare as well as with quasiclassical trajectory calculations of Blais and Truhlar. Although the combined experimental data agree well with the quasiclassical trajectory calculations of Blais and Truhlar, it is suggested that the latter yield rotational distributions which are slightly too hot.

### 1. Introduction

The hydrogen atom exchange reaction  $H+H_2 \rightarrow H_2+H$  (and its isotopic variants) has attracted the interest of many researchers [1]. Being the simplest neutral-neutral bimolecular reaction, very precise theoretical calculations are possible. The H<sub>3</sub> potential energy surface is the best known reactive surface [2]. Both quasiclassical trajectory (QCT) [3,4] and 3-D quantum mechanical calculations [5] have been performed for this system, predicting product quantum state distributions (and other attributes) for collision energies between 0 and 1.6 eV.

In 1983 the first quantum state specific measurements were published independently by two groups. Both groups used HI photolysis to generate translationally hot H atoms for initiating the reaction. For state specific detection, Gerrity and Valentini [6] (GV) employed coherent anti-Stokes Raman spectroscopy (CARS) while Marinero, Rettner and Zare [7] (MRZ) used resonance-enhanced multiphoton ionization (REMPI). The measurements were performed at center-of-mass collision energies of 0.55

and 1.30 eV for the reaction  $H+D_2(v=0, J \text{ thermal}) \rightarrow HD(v, J)+D$ . The overall results of GV and MRZ were in fairly close agreement, but there were deviations outside their combined errors.

Because of these discrepancies we have repeated the measurements for the H+D<sub>2</sub> reaction system at the same collision energies, again using (2+1) REMPI for detection. We report here the HD internal state distributions for  $v=1, J=0-12$  and  $v=2, J=0-8$ , which extend the previously published results. This is the first experimental observation of all of the energetically accessible levels in these two vibrational bands. The experimental setup differs from that of MRZ in several respects and is briefly discussed in this Letter. A more detailed description of the experimental setup is given in refs. [8-10].

### 2. Experimental

A mixture of HI and D<sub>2</sub> (ratio 1 : 3.5) effusively flows from a capillary glass nozzle into a high vacuum chamber (base pressure:  $5 \times 10^{-8}$  Torr). The reagent beam is crossed with two counterpropagating laser beams  $\approx 1$  mm below the nozzle. The first laser (Spectra Physics, DCR-11, Nd : YAG laser, 266 nm (fourth harmonic)) photolyzes the HI. The pho-

<sup>1</sup> Present address: Battelle Pacific Northwest Laboratory, Molecular Science Research Center, MS K2-44/PSL 1529, Richland, WA 99352, USA.

tolysis laser is collimated to  $\approx 2.5$  mm diameter and has a typical pulse energy of  $\approx 3.5$  mJ. The photodissociation generates fast hydrogen atoms with center-of-mass collision energies of 0.55 and 1.3 eV in the concentration ratio 1 : 2, corresponding to the production of the two spin-orbit states,  $I^*(^2P_{1/2})$  and  $I(^2P_{3/2})$ , respectively. Although both hot H atom channels have sufficient energy to overcome the  $\approx 0.42$  eV activation barrier [11] (classical value) for this reaction, only the faster contributes to  $v=2$ . The slower H atoms can result in formation of  $v=1$  product up to  $J=3$ . Their contribution to the sum of the QCT partial cross sections for  $J=0-3$  is only about 9% of the total, but for a particular partial cross section it can be as high as 19% [4].

After a time delay of 50–75 ns, the second laser is fired to detect the HD reaction product. State-specific detection is achieved by (2+1) REMPI. The HD molecule absorbs two photons of  $\approx 200$  nm to undergo the transition from the ground electronic state  $X^1\Sigma_g^+(v, J)$  to the double minimum E,F  $^1\Sigma_g^+(v'=0, J'=J)$  state. Absorption of a subsequent photon of the same wavelength produces  $HD^+$  ions. The ions are formed between the acceleration plates of a shuttered time-of-flight (TOF) mass spectrometer [8] and are injected into the differentially pumped TOF chamber (base pressure:  $3 \times 10^{-8}$  Torr) through a small aperture (3.5 mm wide, 7 mm long). The time-gated ion signal is detected by a chevron multi-channel plate detector and is collected on a computer-interfaced, CAMAC-based data acquisition system [10].

Tunable  $\approx 200$  nm light is obtained by frequency tripling (INRAD, Autotracker II) a Nd:YAG-pumped dye laser (Spectra Physics, DCR-3G/PDL-1; R 640/DCM) using  $\beta$ -barium borate (BBO) crystals<sup>#1</sup>. The probe laser beam (1.0–1.5 mJ) is focused to an estimated 100  $\mu$ m spot size ( $f=125$  mm, plano convex, Suprasil I) into the reaction region. Both beams are horizontally polarized.

In the absence of the photolysis laser,  $HD^+$  ions are still detected [12]. This results from probe laser photolysis of HI. The probe-laser-induced product

signal, which hereafter will be referred to as the prompt signal, must be subtracted from the observed signal in order to obtain the desired distribution because it is not experimentally feasible to saturate the 266 nm photolysis of HI. The correction was made on a shot by shot basis and is described in ref. [9].

The two-photon transition moments, ionization probabilities, and the instrumental function (if any) are not known. A major effort has therefore been directed toward calibrating the detection procedure. Because a room temperature source allows the calibration of only a small portion ( $v=0, J=0-6$ ) of the observed, reactive spectrum ( $v=0, J=0-13; v=1, J=0-12; v=2, J=0-8$ ), a high temperature ( $\leq 1800$  K) oven has been constructed which provides an effusive HD beam. The elevated temperature is required to populate the high rovibrational levels which are observed in the reaction (except  $HD(v=1, J=12)$ ). The comparison of the measured oven gas distribution with a Boltzmann distribution yields any necessary correction factors. The measured and integrated ion signals are then multiplied by these factors to obtain the relative quantum state populations [9,13].

### 3. Results

Several checks were made for systematic errors [9]. From these the following experimental parameters were found to be optimal: an HI :  $D_2$  mix ratio of 1 : 3.5 gave the highest product yield; at a nozzle pressure of 12–15 Torr and a delay of about 55 ns, neither product fly-out nor collisional relaxation occurred to any detectable extent.

The saturation of the ionization step was confirmed at all rotational levels. It is therefore possible to assume that the  $HD^+$  ion signal depends quadratically on the laser power. The signal is corrected for changes in the probe laser intensity caused by the dye gain curve and both short and long term drifts. The validity of the quadratic power correction is verified from studies of the oven calibration spectra.

Oven spectra were taken at different temperatures and pressures of HD. The calibration procedure is described in ref. [9]. The detection scheme is independent of  $J$  for  $HD(v=1, J=0-11)$  and  $HD(v=2, J=0-8)$  and the power-corrected, inte-

<sup>#1</sup> The barium borate crystals were supplied by R.S. Feigelson and R.K. Route and grown as part of a research program sponsored in part by the Army Research Office, contract DAAL03-86-K-0129, and in part by the NSF/MRL Program through the Center for Materials Research, Stanford University.

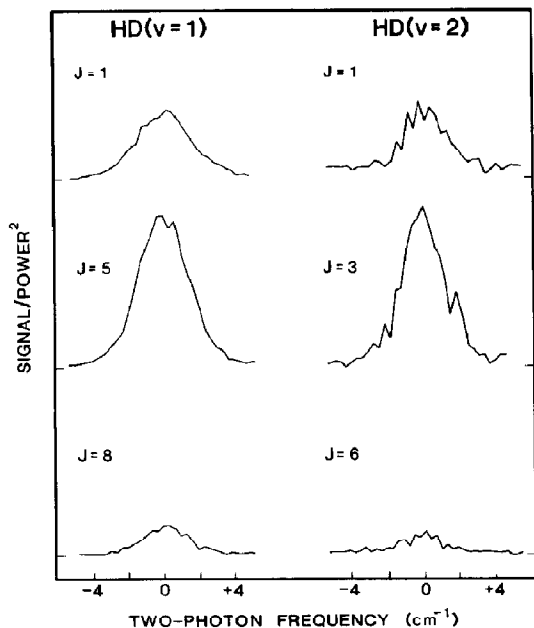


Fig. 1. REMPI signal for product from the  $\text{H} + \text{D}_2$  reaction: (a)  $\text{HD}(v=1, J)$  and (b)  $\text{HD}(v=2, J)$ .

grated ion signals are directly proportional to quantum state populations [9,13]. The observed ion signal of  $\text{HD}(v=2, J=1)$  is contaminated because the line is blended in the  $(2+1)$  REMPI detection scheme [13]. It is reported here but is omitted in the analysis because the degree of the contamination could not be determined.

Some typical reaction spectra are shown in fig. 1. They are taken under the above conditions with the same detector gain and averaged with a 3.5 s time constant.

#### 4. Discussion

The measured HD populations are listed for  $v=1$  and 2 in tables 1 and 2, respectively. For comparison the previously published data sets of MRZ [7], GV [6], and BT [4] are included. As we measure relative populations (not absolute cross sections), the distributions within each vibrational band are normalized to the sum of the populations in all  $J$  levels common with the reported set. Figs. 2–5 show the

Table 1  
HD product quantum state populations<sup>a,b)</sup> for  $\text{H} + \text{D}_2 \rightarrow \text{HD}(v=1, J) + \text{D}$

$J$	This work	MRZ [7]	GV [6]	BT [4]
0	0.019(04)	0.031(02)		0.021(07)
1	0.067(15)	0.075(03)	0.084(11)	0.071(12)
2	0.100(17)	0.134(07)	0.112(11)	0.077(12)
3	0.131(21)	0.145(07)	0.146(22)	0.084(14)
4	0.156(18)	0.161(06)	0.118(22)	0.150(18)
5	0.147(14)	0.129(13)	0.140(11)	0.139(18)
6	0.130(13)	0.075(21)	0.140(11)	0.144(18)
7	0.118(15)		0.090(11)	0.119(18)
8	0.073(15)		0.073(11)	0.107(15)
9	0.034(12)		0.053(11)	0.055(11)
10	0.014(08)			0.029(08)
11	0.006(08)			0.004(03)
12	0.005(07)			0.0004(4)

<sup>a)</sup> Numbers in parentheses represent one standard deviation in the last digits, e.g., 0.019(04) means  $0.019 \pm 0.004$ .

<sup>b)</sup> The distributions are normalized to the sum of the  $(v, J)$  levels common with the reported distribution.

HD quantum state distributions as a function of  $v$  and  $J$  along with various comparisons.

##### 4.1. $\text{HD}(v=1, J)$

Levels up to  $J=12$  are energetically accessible and populations for all  $J$  levels were observed (fig. 2). The distribution peaks at  $J=4$  and falls off slowly to

Table 2  
HD product quantum state populations<sup>a,b)</sup> for  $\text{H} + \text{D}_2 \rightarrow \text{HD}(v=2, J) + \text{D}$

$J$	This work	MRZ [7]	GV [6]	BT [4]
0	0.074(13)	0.052(09)		0.053(20)
1	0.121(28)	0.191(13)		0.133(33)
2	0.193(16)	0.227(21)	0.170(32)	0.147(40)
3	0.215(21)	0.202(20)	0.188(40)	0.147(40)
4	0.193(20)	0.152(28)	0.162(36)	0.173(40)
5	0.121(14)	0.116(19)	0.202(36)	0.213(47)
6	0.058(13)	0.034(12)		0.080(27)
7	0.020(15)			0.073(27)
8	0.006(10)			0.010(07)
9				0.003(01)
10				0.001(01)

<sup>a)</sup> Numbers in parentheses represent one standard deviation in the last digits, e.g., 0.074(13) means  $0.074 \pm 0.013$ .

<sup>b)</sup> The distributions are normalized to the sum of the  $(v, J)$  levels common with the reported distribution.

be just above the noise level for  $J=12$ .

The previous (2+1) REMPI distribution [7] is shown in fig. 2a. Although the rise and the peak positions coincide within the error bars, the falling tail differs. MRZ reported no populations past  $J=6$ . In the present experiment it was possible to detect rotational levels as high as  $J=12$ . There are several causes for this:

(1) The change of the calibration standard: MRZ used a buffered microwave discharge reference source. The excited HD was rotationally relaxed in argon, making calibration impossible for levels higher than  $J=6$ . In the present experiment a high temperature oven is used as the calibration source, allowing the calibration of all the rotational levels (except  $J=12$ ) observed in the reaction.

(2) The increase in the probe laser power has improved the detection sensitivity ( $\approx 1 \times 10^6$  molecules/cm<sup>3</sup> per quantum state), and ensured the saturation of the ionization step.

(3) The shuttered TOF mass spectrometer has substantially increased the signal-to-noise ratio [8].

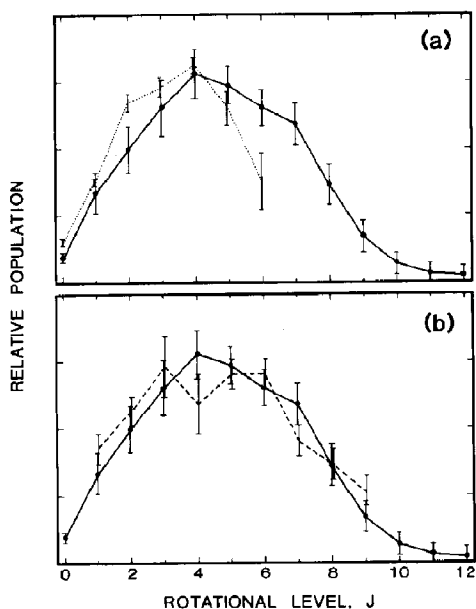


Fig. 2. Rotational distribution of  $\text{HD}(v=1, J)$ . For comparison the experimental results by MRZ [7] (dotted line) and by GV [6] (broken line) are also plotted in (a) and (b), respectively. The data of the present study are shown as symbols connected by a solid line. Both distributions are normalized to the sum of the common  $J$ 's. Error bars represent one standard deviation.

The distribution agrees well with the CARS measurements by GV (fig. 2b). Because of the lower detection sensitivity of CARS, the distribution is reported only for  $J=1-9$ . The error bars of all 9 common points overlap. The four additional levels observed by MPI but not by CARS were not used in the normalization. The shape of the reported MPI distribution is smooth and no evidence was found for the dip at  $J=4$  as seen in the CARS results (in agreement with MRZ). There is precedence for a bimodal distribution in quantum theoretical treatments of  $\text{H} + \text{H}_2$  reactive scattering [14]. The observation that the  $\text{HD}(v=1)$  rotational distribution is not bimodal is therefore significant.

The comparison to the QCT results of BT (fig. 3) is generally good; 11 out of 13 points agree to within the error bars. However, the QCT results seem to be shifted to higher  $J$  by about half a rotational quantum. The first moments are  $\langle J \rangle = 4.78 \pm 0.26$  for the distribution reported here and  $\langle J \rangle = 5.16 \pm 0.27$  for the QCT distribution.

#### 4.2. $\text{HD}(v=2, J)$

The formation of  $\text{HD}(v=2, J)$  is a minor channel for the title reaction. This is evidenced in the significantly lower values of the QCT partial cross sections and the truncated experimental data sets. Energetically, the formation of HD product up to

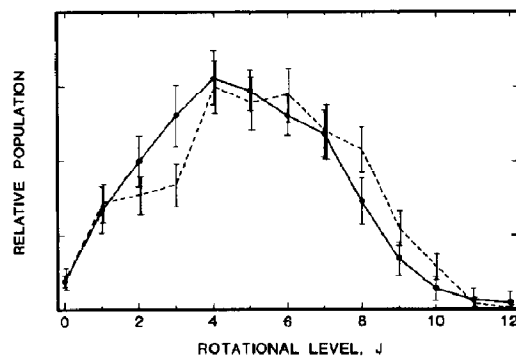


Fig. 3. Comparison of experimental and theoretical  $\text{HD}(v=1, J)$  product distributions. The broken line shows the QCT results calculated by BT [4]; the symbols (connected by a solid line) show the results of the present study. Both distributions are normalized to the sum of the common  $J$ 's. Error bars represent one standard deviation.

$J=8$  is allowed. Population is observed from  $J=0$  to 8 (fig. 4); the population in  $J=8$  is barely detectable within our signal-to-noise ratio. The peak is at  $J=3$ , one  $J$  lower than that of  $v=1$ .

The distribution by MRZ is reported for  $J=0-6$  and shifted to lower  $J$  (fig. 4a) with respect to the present results; it peaks at  $J=2$ . The explanation is as given for  $v=1$ .

CARS data are reported for 4 out of the 9 populated rotational levels with error bars of 18–22%. A meaningful comparison with the data of GV is therefore not possible (fig. 4b).

The QCT distribution for  $v=2$  peaks abruptly at  $J=5$  and cuts off sharply at  $J=8$  (fig. 5). The uncertainties in the calculated populations are in excess of 20% because of the small number of trajectories that resulted in the formation of HD( $v=2$ ). Nonetheless, the QCT distribution again appears to be rotationally too hot. The first moment of the reported distribution is  $\langle J \rangle = 3.06 \pm 0.18$ , while that for the QCT calculation is  $\langle J \rangle = 3.61 \pm 0.40$ .

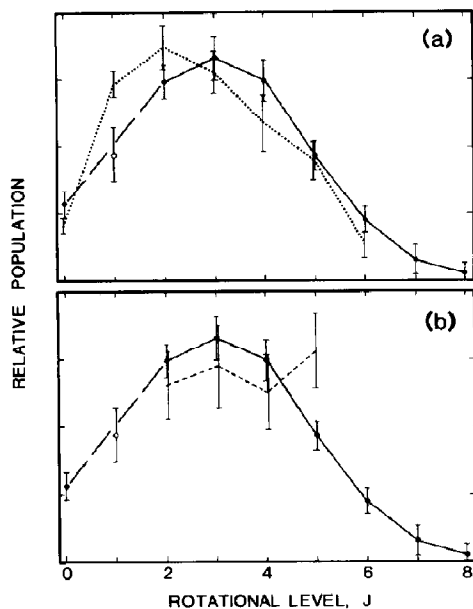


Fig. 4. Rotational distribution of HD( $v=2, J$ ). For comparison the experimental results by MRZ [7] (dotted line) and by GV [6] (broken line) are plotted in (a) and (b), respectively. The data of the present study are shown as symbols connected by a solid line. Both distributions are normalized to the sum of the common  $J$ 's. Error bars represent one standard deviation.

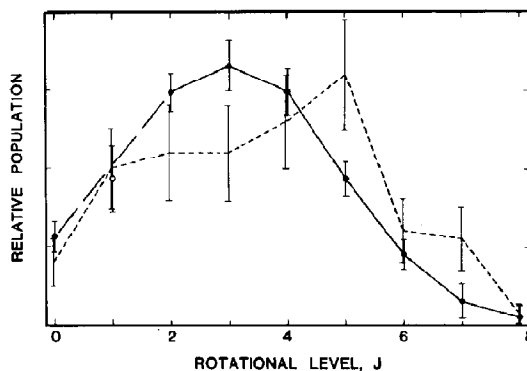


Fig. 5. Comparison of experimental and theoretical HD( $v=2, J$ ) product distributions. The broken line shows the QCT results calculated by BT [4]; the symbols (connected by a solid line) show the results of the present study. Both distributions are normalized to the sum of the common  $J$ 's. Error bars represent one standard deviation.

The improvements in the experimental setup permitted the measurement of all of the energetically allowed rovibrational levels of HD( $v=1, 2$ ). Based on the average QCT partial cross section [4] for HD( $v=1, J=11, 12$ ) and HD( $v=2, 8$ ) the smallest detectable cross section for the present experimental setup is  $\approx 5 \times 10^{-4} \text{ \AA}^2$ . The earlier MPI rotational distributions appear to be slightly too cold for both  $v=1, 2$ . The experimental and quasiclassical results agree well overall. However, based on the excellent agreement between the CARS and REMPI  $v=1$  distributions, we are encouraged to suggest that the QCT rotational distributions are slightly too hot. This trend was also observed by Schatz [5] in comparing his three-dimensional quantum mechanical calculations with QCT calculations at a lower collision energy (0.55 eV).

#### Acknowledgement

We thank T.A. Stephenson for early work on this system and are grateful to A.C. Kummel and G.O. Sitz for many useful discussions. We thank L. Wolford for technical assistance with the laser system. Graduate fellowships are gratefully acknowledged by K-DR (Deutscher Akademischer Austauschdienst, Jahresstipendium 1984/5; Rotary Foundation, 1985/6) and DAVK (National Science

Foundation, 1986-89). This project is supported by the National Science Foundation under Grant No. NSF CHE 87-05131.

## References

- [1] F. London, *Z. Elektrochem.* 35 (1929) 552;  
H. Eyring and M. Polanyi, *Z. Physik. Chem. B* 12 (1931) 279;  
D.G. Truhlar and R.E. Wyatt, *Ann. Rev. Phys. Chem.* 27 (1976) 1, and references therein;  
*Intern. J. Chem. Kinetics* 18, No. 9 (1986).
- [2] B. Liu, *J. Chem. Phys.* 68 (1973) 1925;  
P. Siegbahn and B. Liu, *J. Chem. Phys.* 68 (1978) 2457;  
D.G. Truhlar and C.J. Horowitz, *J. Chem. Phys.* 68 (1978) 2466; 71 (1978) 1514;  
A.C. Varandas, F.B. Brown, C.A. Mead, D.G. Truhlar and N.C. Blais, *J. Chem. Phys.* 86 (1987) 6258.
- [3] N.C. Blais, D.G. Truhlar and B.C. Garrett, *J. Chem. Phys.* 82 (1985) 2300;  
N.C. Blais and D.G. Truhlar, *J. Chem. Phys.* 83 (1985) 2201; 88 (1988) 5457.
- [4] N.C. Blais and D.G. Truhlar, *Chem. Phys. Letters* 102 (1983) 120.
- [5] G.C. Schatz, *Chem. Phys. Letters* 108 (1984) 53;  
M.C. Colton and G.C. Schatz, *Chem. Phys. Letters* 124 (1986) 256;  
C.R. Klein and S.H. Suck Salk, *Chem. Phys. Letters* 125 (1986) 481;  
F. Webster and J.C. Light, *J. Chem. Phys.* 85 (1986) 4744;  
A. Kuppermann and P.G. Hipes, *J. Chem. Phys.* 84 (1986) 5962;  
P.G. Hipes and A. Kuppermann, *Chem. Phys. Letters* 133 (1986) 1.
- [6] D.P. Gerrity and J.J. Valentini, *J. Chem. Phys.* 79 (1983) 5202; 81 (1984) 1298.
- [7] C.T. Rettner, E.E. Marinero and R.N. Zare, in: *Physics of Electronic and Atomic Collisions. Invited Papers from the XVIIIth ICPEAC, Berlin, July 27-Aug. 2, 1983*, eds. J. Eichler, I.V. Hertel and N. Stolterfoht (North-Holland, Amsterdam, 1984) p. 51;  
E.E. Marinero, C.T. Rettner and R.N. Zare, *J. Chem. Phys.* 80 (1984) 4141.
- [8] K.-D. Rinnen, D.A.V. Kliner, R.S. Blake and R.N. Zare, *Rev. Sci. Instr.*, submitted for publication.
- [9] K.-D. Rinnen, D.A.V. Kliner, R.S. Blake and R.N. Zare, *J. Chem. Phys.*, to be submitted for publication.
- [10] R.S. Blake, Ph.D. Thesis, Department of Chemistry, Stanford University, Stanford (1988).
- [11] B. Liu, *J. Chem. Phys.* 80 (1984) 581;  
D.M. Ceperley and B.J. Alder, *J. Chem. Phys.* 81 (1984) 5833;  
R.N. Barnett, P.J. Reynolds and W.A. Lester Jr., *J. Chem. Phys.* 82 (1985) 2700.
- [12] K.-D. Rinnen, D.A.V. Kliner, R.S. Blake and R.N. Zare, *Chem. Phys. Letters* 153 (1988) 371.
- [13] K.-D. Rinnen, D.A.V. Kliner, R.N. Zare and W.M. Huo, *Israel J. Chem.*, to be submitted for publication.
- [14] F. Webster and J.C. Light, *J. Chem. Phys.*, to be published.